Cardiovascular Research (2011) **89**, 60–71
doi:10.1093/cvr/cvq288

Cardiac-specific leptin receptor deletion exacerbates ischaemic heart failure in mice

Kenneth R. McGaffin[1]*, William G. Witham[1], Keith A. Yester[1], Lia C. Romano[2], Robert M. O'Doherty[3], Charles F. McTiernan[1], and Christopher P. O'Donnell[2]

[1]Cardiovascular Institute, University of Pittsburgh Medical Center, 1750 Bioscience Tower, 200 Lothrop Street, Pittsburgh, PA 15213, USA; [2]Division of Pulmonary, Allergy, and Critical Care Medicine, University of Pittsburgh Medical Center, Pittsburgh, PA, USA; and [3]Division of Endocrinology and Metabolism, University of Pittsburgh Medical Center, Pittsburgh, PA, USA

Received 28 April 2010; revised 27 August 2010; accepted 1 September 2010; online publish-ahead-of-print 9 September 2010

Time for primary review: 22 days

Aims The obesity-related adipokine, leptin, has multiple actions on peripheral organs, including the mitigation of adverse cardiovascular outcomes after myocardial infarction (MI). Although we recently demonstrated that leptin, its receptor, and downstream signalling are up-regulated in the heart after MI, the significance of intact cardiomyoctye leptin signalling is unknown. Therefore, our objective was to generate a cardiomyocyte-specific leptin receptor knock-out (ObRKO) mouse to determine whether worse cardiac outcomes after MI result from impaired leptin signalling in cardiomyocytes.

Methods and results Tamoxifen-inducible ObRKO mice were subjected to experimental MI or sham surgeries and studied after 1 month. After MI, ObRKO mice displayed a loss of cardiac signal transducer and activator of transcription (STAT) 3 and adenosine monophosphate-activated protein kinase (AMPK) signalling. Worse survival and cardiac morbidity were also seen in the ObRKO mouse post-MI, including decreased contractile function and glycolytic metabolism, and increased left ventricular dilation, hypertrophy, collagen deposition, matrix metalloproteinase activity, apoptosis, and inflammation. Treatment of ObRKO mice post-MI with an ObR-independent AMPK activator improved cardiac function and restored many of these maladaptive processes to wild-type levels.

Conclusion These data indicate that leptin signalling mitigates cardiac injury in the post-MI failing heart by acting directly on cardiomyocytes to increase STAT3 and AMPK activation, to decrease cardiac hypertrophy, apoptosis, and inflammation, and to limit deleterious changes in cardiac structure, function, and glycolytic metabolism.

Keywords Leptin • Heart failure • Cre-lox • Apoptosis • Metabolism

1. Introduction

Adipose tissue produces and secretes a number of substances that act centrally to regulate appetite, metabolism, and cellular physiology.[1] Many of these 'adipokines' also mediate effects directly in peripheral tissues through membrane bound receptors. Within the heart, the adipokine leptin and its receptor (ObR) are abundantly expressed in cardiomyocytes.[2,3] Leptin can regulate the baseline physiology of the heart, including myocyte contractility,[4] hypertrophy,[5] apoptosis,[6] and metabolism.[7,8] During pathological states of myocardial infarction (MI)[9] and heart failure,[10] circulating leptin is increased, most likely from fat-derived sources. However, we have recently shown that increased expression of leptin and its receptor can occur locally in the failing human heart.[3] Moreover, we demonstrated in an experimental murine model of MI that whole-body leptin deficiency results in impaired cardiac structure, function, and survival[2,11] and that the phenotype can be rescued by the systemic repletion of leptin. However, the question remains as to whether the beneficial effects of leptin repletion in the setting of MI are dependent on leptin signalling in cardiomyocytes or secondary to the multiple effects of leptin peripheral to the heart.

Thus, the first goal of our study was to determine whether or not the cardiac-specific disruption of ObR expression, through the development of a mouse with inducible excision of the ObR gene, impacted on cardiac outcomes after MI. We hypothesized that a loss of cardiomyocyte-specific ObR expression would lead to greater decrements in cardiac structure and function, as well as increased myocardial apoptosis, inflammation, and hypertrophy,

* Corresponding author. Tel: +1 412 647 2345; fax: +1 412 383 8857, Email: mcgaffinkr@upmc.edu

post-MI. The second goal of our study was to establish whether or not the disruption of cardiac ObR expression also impairs activation of downstream signalling pathways that are known to provide cardioprotective benefit in MI, including signal transducer and activator of transcription (STAT) 3 and adenosine monophosphate-activated protein kinase (AMPK). In particular, since it is known that AMPK is a key regulator of cardiac substrate metabolism,[12] we further hypothesized that the ability of the ischaemic, failing heart to anaerobically metabolize glucose is dependent on an intact ObR-AMPK signalling axis.

2. Methods

2.1 Animals

All animal use conformed with the Guide for the Care and Use of Laboratory Animals published by the US National Institutes of Health (NIH Publication No. 85-23, revised 1996) and was approved by the Institutional Animal Care and Use Committee at the University of Pittsburgh. Previously characterized mice harbouring the floxed ObR gene[13] were a gift of Dr Jeff Friedman (Rockefeller University, NY, USA) and were bred into a pure C57BL/6J background for 8+ generations prior to subsequent breeding with mice homozygous for the α-myosin heavy chain promoter driven MerCreMer transgene (Jackson Laboratories, USA, B6129SF1/J background, stock #005650). Subsequent inbreeding generated double homozygous (+/+) mice for the MerCreMer transgene and the ObR floxed allele. To induce cardiac-specific ObR excision, 8-week-old male MerCreMer$^{+/+}$ ObR floxed$^{+/+}$ (ObRKO) transgenic mice were treated with tamoxifen [tam; 20 mg/kg intraperitoneal (ip)] daily for 7 days, whereas vehicle (oil)-treated control mice received an equivalent volume of 95% peanut oil/5% ethanol. One week after oil or tam treatment, mice were subjected to open thoracotomy and a suture was placed around the left anterior descending coronary artery and left loose (sham procedure) or tightly tied (CAL procedure) as previously described[2] and detailed in the Supplementary material online. All surviving mice were studied at 1-month post-surgery by echocardiography and by an *in vivo* conductance catheter, followed by either tissue collection for biochemical studies, or *ex vivo* perfusion of the heart for glycolytic measurements. For histological and biochemical analyses, seven groups of mice were examined and included two groups of sham mice: (i) vehicle ($n = 16$)- and (ii) tam ($n = 16$)-treated ObRKO; and five groups of CAL mice: (iii) vehicle-treated ObRKO ($n = 16$), (iv) tam-treated ObRKO ($n = 14$), (v) tam-treated parental MerCreMer$^{+/+}$ ($n = 16$), and (vi) tam-treated parental ObR floxed$^{+/+}$ ($n = 15$) and tam-treated ObRKO administered the leptin-independent AMPK activator, aminoimidazole carboxamide ribonucleotide (AICAR), at a dose of 0.5 mg/g ip daily starting at 3 days prior to animal sacrifice ($n = 9$). In a separate set of experiments, an additional five (for sham groups) or eight (for CAL groups) mice were examined per group for cardiac glycolytic metabolism. Finally, an additional set of ObRKO mice were treated with oil ($n = 10$) or tam ($n = 10$), subjected to CAL, and administered leptin ($n = 5$ per tam/oil group at a dose of 0.3 mg/kg ip) or equal volume saline ($n = 5$ per tam/oil group) after 1 month, followed by animal sacrifice 30 min later.

2.2 Genotyping

DNA extraction from tissue was accomplished using the Extract-N-Amp kit (Sigma Aldrich, USA) per manufacturer's instructions. Primers and PCR conditions used are detailed in the Supplementary material online. PCR products were visualized using agarose gel electrophoresis.

2.3 Echocardiography

Parasternal short-axis B- and m-mode images were obtained on mice under 1–2% isoflurane anaesthesia using a Visualsonics echocardiography machine as previously described[2] and detailed in the Supplementary material online.

2.4 *In vivo* pressure–volume loops

At 1-month post-CAL/sham surgeries, left ventricular pressure–volume loops were recorded using Chart and Scope software version 5.4.2 (AD Instruments, USA), an MPVS-400 system (Millar Instruments, USA), and a 1.4 F PV catheter (Millar Instruments). A minimum of five time points per animal (6–10 loops/time point) were analysed and averaged during steady state using PVAN version 3.6 software (Millar) as previously described[14] and detailed in the Supplementary material online.

2.5 *Ex vivo* cardiac perfusion

Hearts were quickly excised, aortas cannulated, and subjected to perfusion with a modified Krebs buffer containing ^{3}H-glucose. ^{3}H-water in collected perfusate samples was separated from ^{3}H-glucose by ion exchange as described by Lopaschuk and Barr,[15] and steady-state calculations were adjusted for the volume of perfusate collected per unit time to determine glycolytic rate. Buffer composition and additional experimental details are provided in the Supplementary material online.

2.6 Quantitative real-time RT–PCR analysis

Total RNA was isolated from whole heart homogenates and subjected to quantitative PCR, as previously described,[2] and detailed in the Supplementary material online.

2.7 Western blotting/zymography

Protein was extracted from whole heart homogenates in RIPA buffer and subjected to SDS–PAGE in equal amounts as described previously.[2] Antibodies and incubation conditions used are detailed in the Supplementary material online.

2.8 Immunofluorescence/histology

Mouse cardiac sections were used for ObR, TUNEL, CD45, α-actinin, picrosirius-red, phalloidin, and H&E stains as previously described[2] and detailed in the Supplementary material online. The determination of apoptotic and inflammatory indices, as well as collagen fractional area, was accomplished using the image analysis software Metamorph v7.5 (Molecular Devices, USA).

2.9 Determination of infarct size, cardiomyocyte area, and width

Mouse cardiac sections were stained with FITC-linked wheat germ agglutinin (to visualize cell membranes) and DAPI (to visualize nuclei) or H&E, and the determination of infarct area and cardiomyocyte dimensions was accomplished using Image J software (NIH), all as previously described,[2] and detailed in the Supplementary material online.

2.10 *In vitro* caspase-3 activity assay

Caspase-3 activity was determined using whole heart homogenates and the caspase-3/CPP32 Colorimetric Assay kit (Biovision, USA) as previously described[11] and detailed in the Supplementary material online.

2.11 Statistics

Data presented are mean ± standard error of the mean (SEM). Statistical significance of mean changes was determined by ANOVA with *post hoc* comparisons between means using Bonferrroni's simultaneous tests. Mathematical calculations, determination of *P* values, Student's *t*-tests, ANOVAs, and the Kaplan–Meier log-rank survival statistics and survival graph were generated using the computer program Statistical Package for the Social Sciences (SPSS) v17 (SPSS, USA).

3. Results

3.1 Tam administration to homozygous MerCreMer ObR floxed mice results in cardiac-specific ObR gene excision

After 7 days of tam treatment, mice homozygous for both MerCreMer$^{+/+}$ and ObR floxed$^{+/+}$ alleles (ObRKO mice) demonstrated excision of the floxed ObR gene in cardiac tissue only (*Figure 1A*). This was accompanied by a reduction in cardiac ObR mRNA and protein expression to 14 $\pm$ 3 and 13 $\pm$ 1% of oil-treated control levels, respectively (*Figure 1B*). Immunofluorescent examination of cardiac sections showed a marked reduction in ObR expression in cardiomyocytes (see Supplementary material online, *Figure S1A*). All mice maintained a lean phenotype and demonstrated no confounding tam effects[16] on cardiac structure and function after tam treatment, with mean end-diastolic dimensions (EDDs), end-diastolic volumes (EDVs), average wall thicknesses, left ventricular ejection fractions, fractional shortenings (FSs), and developed pressures unchanged in sham mice after 7 days of tam treatment relative to oil treatment (*Tables 1* and *2*; see Supplementary material online, *Figure S1B*).

3.2 Cardiac-specific reduction in ObR expression results in a loss of cardiac STAT3 and AMPK signalling at 1-month post-MI

We have previously established that cardiac ObR expression and STAT3 signalling are increased in wild-type mice at 1-month post-MI.[2] Here, we again utilized STAT3 phosphorylation as a read-out of leptin signalling[17] and also examined the phosphorylation state of AMPK. The cardiac expression of total (t) and phosphorylated (p) STAT3 (*Figure 2A*) and AMPK (*Figure 2B*) was unchanged in tam-treated sham mice relative to oil-treated controls. All groups of CAL mice demonstrated an approximately two-fold increase in t-STAT3 and t-AMPK expression; however, only vehicle-treated ObRKO mice, and their corresponding tam-treated parental control mice, demonstrated a significant increase in the ratio of p/t-STAT3 and -AMPK post-MI. With cardiac-specific reduction in ObR expression, tam-treated ObRKO mice demonstrated a significant reduction in p/t-STAT3 and -AMPK relative to all other groups post-MI. Moreover, acute administration of exogenous leptin at 1-month post-MI activated cardiac STAT3 (see Supplementary material online, *Figure S2A*) and AMPK (see Supplementary material

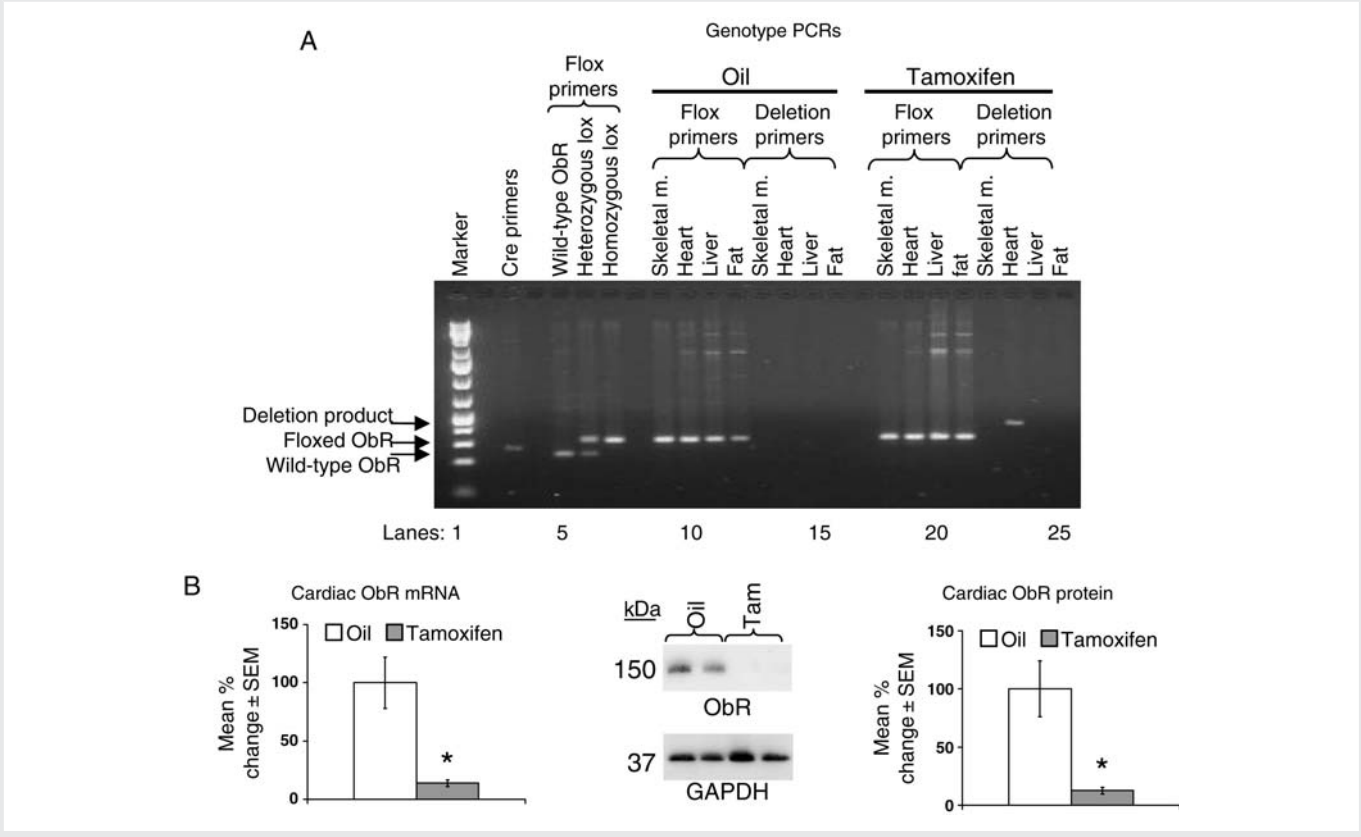

Figure 1 Cardiac-specific ObR deletion and reduction in ObR expression are seen in ObRKO mice after tam treatment. (*A*) Representative agarose gel electrophoresis demonstrating PCR amplification of DNA from the tail, skeletal muscle, heart, liver, and fat from oil-treated and tam-induced ObRKO mice using cre, floxed, and deletion primer pairs. (*B*) Mean $\pm$ SEM fold change in cardiac ObR mRNA (left panel) and protein (right panel) from oil-treated and tam-induced ObRKO mice is shown, along with a representative western blot image showing two samples/group (middle panel). *$P < 0.05$ vs. oil.

Table 1 Mean ± SEM weight and echocardiographic measurements on oil-treated and tam-induced ObRKO sham and CAL mice, and on tam-treated parental MerCreMer$^{+/+}$ and ObR flox$^{+/+}$ CAL mice, at 1-month post-surgery

Group	Body weight (g)	Heart weight (g)	Heart/body weight (ratio × 10^3)	Lung weight (g)	Wet/dry lung weight (ratio)	Fractional shortening (%)	End-diastolic dimension (mm)	End-systolic dimension (mm)	Average wall thickness (mm)	Heart rate (b.p.m.)
ObRKO oil sham ($n = 16$)	25.1 ± 0.5	0.121 ± 0.002	4.82 ± 0.10	0.133 ± 0.003	3.69 ± 0.11	50.4 ± 0.8	2.98 ± 0.03	1.48 ± 0.03	0.95 ± 0.01	519 ± 12
ObRKO tam sham ($n = 16$)	25.2 ± 0.7	0.119 ± 0.002	4.72 ± 0.10	0.131 ± 0.003	3.79 ± 0.07	50.9 ± 0.4	3.04 ± 0.04	1.49 ± 0.04	0.97 ± 0.01	541 ± 18
ObRKO oil CAL ($n = 16$)	24.7 ± 0.5	0.135 ± 0.004*	5.46 ± 0.11*	0.151 ± 0.004*	4.19 ± 0.05*	27.2 ± 0.6*	4.56 ± 0.05*	3.32 ± 0.15*	1.11 ± 0.01*	520 ± 12
ObRKO tam CAL ($n = 14$)	25.6 ± 0.6	0.155 ± 0.003†	6.05 ± 0.10†	0.172 ± 0.006†	4.63 ± 0.11†	19.4 ± 0.4†	4.99 ± 0.06†	4.02 ± 0.06†	1.21 ± 0.02†	510 ± 10
MerCreMer$^{+/+}$ tam CAL ($n = 16$)	24.2 ± 0.8	0.132 ± 0.005*	5.45 ± 0.11*	0.146 ± 0.005*	4.26 ± 0.10*	27.3 ± 0.9*	4.38 ± 0.15*	3.19 ± 0.06*	1.10 ± 0.01*	519 ± 10
ObR floxed$^{+/+}$ tam CAL ($n = 15$)	24.3 ± 0.8	0.134 ± 0.002*	5.51 ± 0.12*	0.148 ± 0.003*	4.11 ± 0.09*	28.5 ± 0.7*	4.44 ± 0.14*	3.17 ± 0.05*	1.10 ± 0.01*	520 ± 6
ObRKO tam CAL + AICAR ($n = 9$)	24.5 ± 0.7	0.141 ± 0.003#	5.75 ± 0.18#	0.157 ± 0.002#	4.45 ± 0.03#	24.3 ± 1.3#	4.62 ± 0.05#	3.49 ± 0.07#	1.16 ± 0.01#	523 ± 9

*$P < 0.05$ vs. shams.
†$P < 0.05$ vs. all groups.
#$P < 0.05$ vs. ObRKO tam CAL.

Table 2 Mean ± SEM cardiac functional data derived from *in vivo* pressure–volume loops on oil-treated and tam-induced ObRKO sham and CAL mice, and on tam-treated parental MerCreMer$^{+/+}$ and ObR floxed$^{+/+}$ CAL mice at 1-month post-surgery

Group	Ejection fraction (%)	Cardiac output (μL/min)	Stroke volume (μL)	Stroke work (mmHg/μL)	End-diastolic volume (μL)	End-systolic volume (μL)	Heart rate (b.p.m.)	dP/dt_{max} (mmHg/s)	dP/dt_{min} (mmHg/s)
ObRKO oil sham ($n = 16$)	55.3 ± 1.3	9742 ± 634	20.6 ± 1.2	1763 ± 142	36.8 ± 2.6	16.2 ± 1.4	473 ± 12	11 445 ± 504	−10 625 ± 589
ObRKO tam sham ($n = 16$)	55.6 ± 1.4	9650 ± 514	20.1 ± 1.1	1689 ± 85	36.5 ± 2.7	16.4 ± 1.7	480 ± 10	12 026 ± 720	−10 694 ± 547
ObRKO oil CAL ($n = 16$)	23.8 ± 1.0*	8061 ± 638*	16.9 ± 1.3*	986 ± 90*	70.3 ± 4.2*	53.4 ± 3.6*	477 ± 12	6901 ± 180*	−6333 ± 185*
ObRKO tam CAL ($n = 14$)	14.6 ± 0.6†	5783 ± 288†	12.3 ± 0.6†	634 ± 40†	81.9 ± 3.6†	69.6 ± 3.4†	470 ± 12	4983 ± 194†	−4974 ± 244†
MerCreMer$^{+/+}$ tam CAL ($n = 16$)	23.8 ± 0.9*	8132 ± 382*	16.7 ± 0.2*	932 ± 72*	70.5 ± 3.3*	53.8 ± 3.2*	487 ± 8	7008 ± 180*	−6576 ± 155*
ObR floxed$^{+/+}$ tam CAL ($n = 15$)	24.6 ± 1.0*	7954 ± 468*	16.2 ± 1.0*	992 ± 102*	71.0 ± 5.0*	54.8 ± 4.5*	491 ± 12	6824 ± 472*	−6399 ± 421*
ObRKO tam CAL + AICAR ($n = 9$)	21.5 ± 0.4$^{\#}$	7505 ± 652$^{\#}$	15.8 ± 1.4$^{\#}$	999 ± 78$^{\#}$	73.4 ± 1.4$^{\#}$	57.6 ± 2.8$^{\#}$	475 ± 9	6553 ± 592$^{\#}$	−5357 ± 591$^{\#}$

*$P < 0.05$ vs. shams.
$^{\dagger}P < 0.05$ vs. all groups.
$^{\#}P < 0.05$ vs. ObRKO tam CAL.

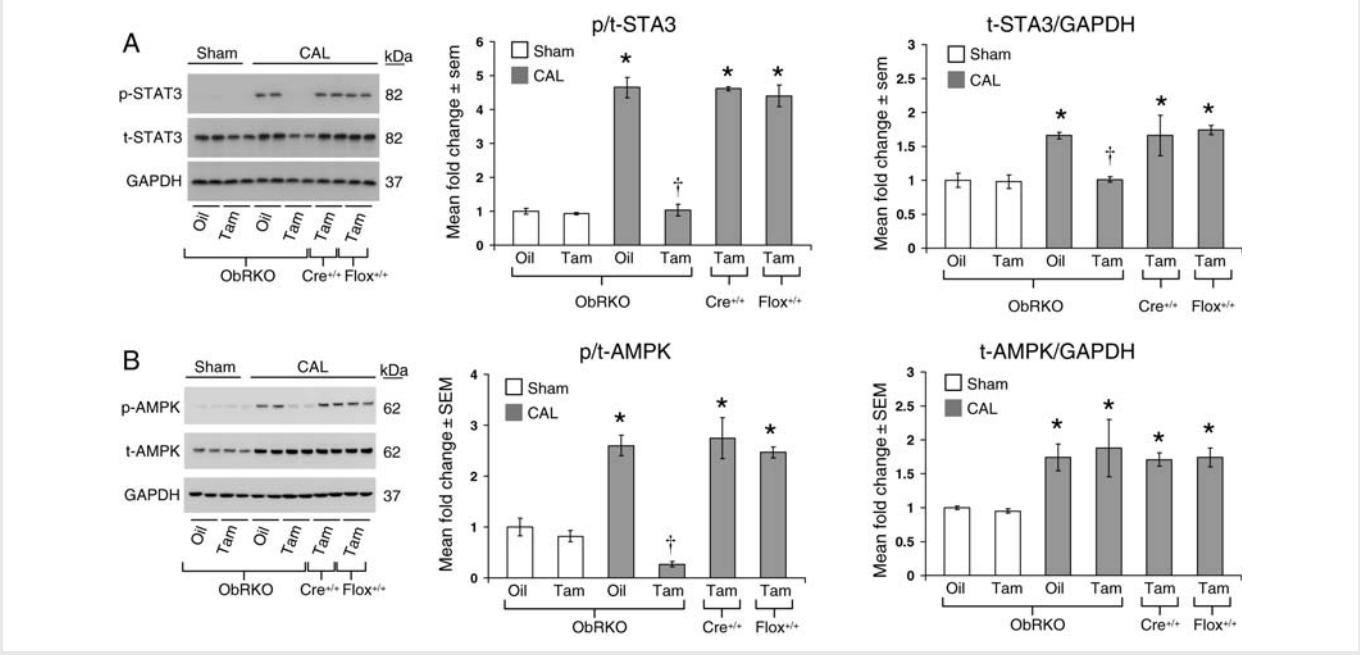

Figure 2 Tam-induced ObRKO mice demonstrate a loss of cardiac STAT3 and AMPK activation post-MI. $^{*}P < 0.05$ vs. shams, $^{\dagger}P < 0.05$ vs. all CAL groups. (*A*) Mean ± SEM fold change in cardiac p/t-STAT3 (middle panel) and t-STAT3/GAPDH (right panel) in various groups of ObRKO and homozygous (+/+) parental MerCreMer ($Cre^{+/+}$) and floxed ($flox^{+/+}$) mice is shown, along with representative western blot showing two samples/group (left panel). (*B*) As in (A), except that the data for Thr172-p/t-AMPK and t-AMPK/GAPDH are shown.

online, *Figure S2B*) only in oil-treated ObRKO mice. In control experiments, both total and p/t-STAT3 and -AMPK in tam-treated parental $MerCreMer^{+/+}$ and ObR $floxed^{+/+}$ mice were not significantly different from oil-treated ObRKO mice post-MI (*Figure 2A* and *B*).

3.3 Cardiac-specific reduction in ObR expression exacerbates indices of heart failure that are rescued with AMPK activation at 1-month post-MI

At one-month post-surgery, survival in sham mice was 100% (32/32). With CAL, 80% survival (16/20) was seen in oil-treated ObRKO mice, which was not different than survival in tam-treated $MerCreMer^{+/+}$ (16/20) and ObR $floxed^{+/+}$ (15/18) parental mice, but was significantly better than the 46% survival (14/30) seen in tam-treated ObRKO mice (*Figure 3E*). Despite equal infarct areas in oil- and tam-treated ObRKO mice (6.35 ± 0.26 vs. 6.31 ± 0.28 mm^2, $P > 0.05$; see Supplementary material online, *Figure S3*), both heart and lung weights of tam-treated ObRKO mice were significantly increased, and tam-treated ObRKO mice subjected to CAL demonstrated the greatest increase in EDD and end-systolic dimension, and the greatest decrease in per cent FS, at 3-day, 1-, 2-, and 3-week, and 1-month post-surgery (see Supplementary material online, *Figure S4* and *Table S1*; *Table 1* and *Figure 3A*). These exacerbated indices of heart failure in the tam-treated ObRKO mouse post-MI were consistent with pressure–volume data at 1-month post-MI, which demonstrated significant increases in EDV and end-systolic volume, and significant decreases in cardiac output, ejection fraction, and developed pressures (*Table 2* and *Figure 3B*). With each measured outcome, tam-treated homozygous (+/+) MerCreMer ($Cre^{+/+}$) and floxed ($flox^{+/+}$) parental mice demonstrated changes in cardiac structure and function at 1-month post-MI that were no different than oil-treated ObRKO mice post-MI (*Tables 1* and *2* and *Figure 3A* and *B*). Consistent with the literature,[18,19] AICAR administration resulted in the activation of cardiac AMPK (*Figure 3C*), and significant improvements in both echocardiographic- and pressure–volume-determined indices of heart failure were observed (*Figure 3D*, and *Tables 1* and *2*).

3.4 Cardiac-specific reduction in ObR expression results in greater indices of biochemical remodelling that are rescued with AMPK activation at 1-month post-MI

The cardiac mRNA expression of atrial naturetic peptide (ANP), brain naturetic peptide (BNP), β-myosin heavy chain (βMHC), interleukin (IL)-1β, and tumour necrosis factor α (TNFα) were all increased post-MI in tam-treated ObRKO mice, whereas IL10 mRNA was decreased (*Figure 4A*, see Supplementary material online, *Table S2*). Further, both myocyte width and area (*Figure 4B*; see Supplementary material online, *Figure S5*), as well as echocardiographic determination of wall thicknesses (*Figure 3A* and *Table 1*), were increased post-MI in tam relative to oil-treated ObRKO mice, or tam-treated homozygous (+/+) MerCreMer ($Cre^{+/+}$) and floxed ($flox^{+/+}$) parental mice. Moreover, increased deposition of collagen was observed in cardiac sections from tam-treated ObRKO mice (*Figure 4C*; see Supplementary material online, *Figure S6*) and correlated with increased zymographically determined matrix metalloproteinase (MMP) 2 and 9 activity (*Figure 4D*). With AICAR administration, tam-treated ObRKO mice demonstrated significant reductions in foetal gene and inflammatory cytokine mRNA expression, myocyte hypertrophy, collagen deposition, and MMP activity (*Figure 4A–D*, *Table 1*; see Supplementary material online, Figures *S5* and *S6*).

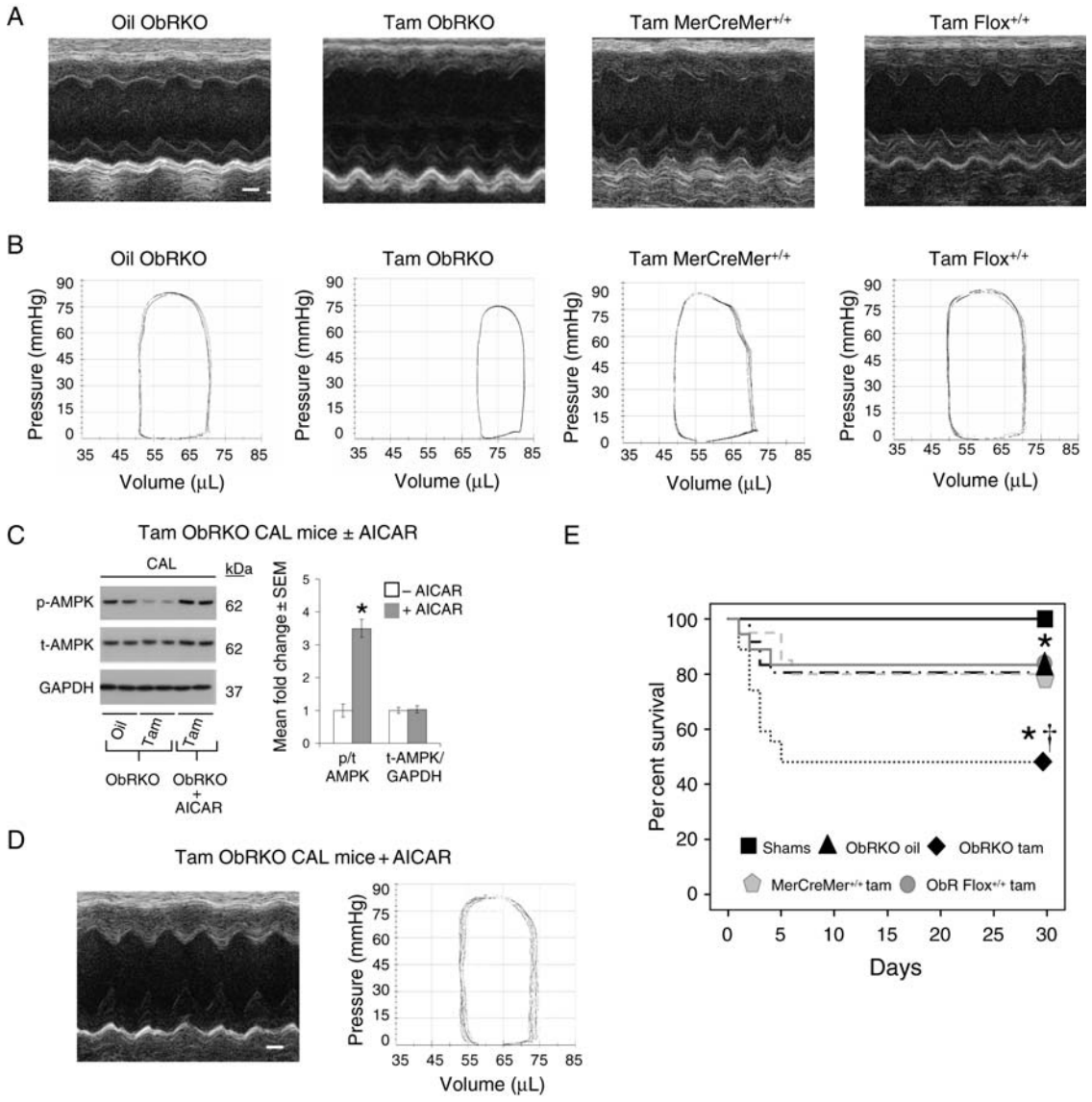

Figure 3 Tam-induced ObRKO mice demonstrate worse survival and greater decrements in cardiac structure and function post-MI. *$P < 0.05$ vs. shams and $^{\dagger}P < 0.05$ vs. all CAL groups. (*A*) Representative m-mode echocardiographic images from oil-treated ObRKO mice (left panel), and tam-treated ObRKO (second panel) and homozygous (+/+) parental MerCreMer ($Cre^{+/+}$) and floxed ($flox^{+/+}$) mice (right two panels), with accompanying scale bar (1 mm) shown in white. (*B*) As in (A), except that the pressure–volume loops are shown. (*C*) Mean ± SEM fold change in cardiac p/t-AMPK (middle panel) and t-AMPK/GAPDH (right panel) in tam-treated ObRKO CAL mice 3 days after administration of AICAR, along with representative western blot showing two samples/group (left panel). (*D*) Representative echocardiographic and pressure–volume data from a tam-treated ObRKO mouse administered AICAR post-MI. (*E*) Thirty-day Kaplan–Meier survival plot of sham (ObRKO oil- and tam-treated groups combined) and CAL mice (oil- and tam-treated ObRKO, and tam-treated homozygous parental MerCreMer$^{+/+}$ and ObR Flox$^{+/+}$ mice).

3.5 Cardiac-specific reduction in ObR expression results in greater cardiomyocyte apoptosis, inflammation, and caspase-3 activity that are rescued with AMPK activation at 1-month post-MI

Hearts from both oil- and tam-treated ObRKO mice subjected to sham procedure demonstrated comparable rates of total apoptosis (~0.09%), inflammation (i.e. the per cent of nuclei that are CD45+, ~4%), and TUNEL/α-actinin-positive cells (~0.05%; *Figure 5A–F*). Additionally, in control experiments, rates of apoptosis, inflammation, and TUNEL/α-actinin-positive cells in hearts from homozygous (+/+) MerCreMer ($Cre^{+/+}$) and floxed ($flox^{+/+}$) parental lines of mice treated with tam and subjected to CAL were not significantly different from each other, or oil-treated ObRKO mice (all $P > 0.05$; *Figure 5A–F*). However, increased indices of inflammation and apoptosis were seen in both remote and infarcted myocardium from ObRKO mice with cardiomyocyte-specific reduction in ObR expression (*Figure 5A–F*). Specifically, relative to oil-treated mice, remote tissue from tam-treated ObRKO mice subjected to CAL demonstrated significantly greater levels of total TUNEL-positive (~0.58 vs. ~0.16%; $P < 0.05$), CD45-positive (~26 vs. ~20%; $P <$

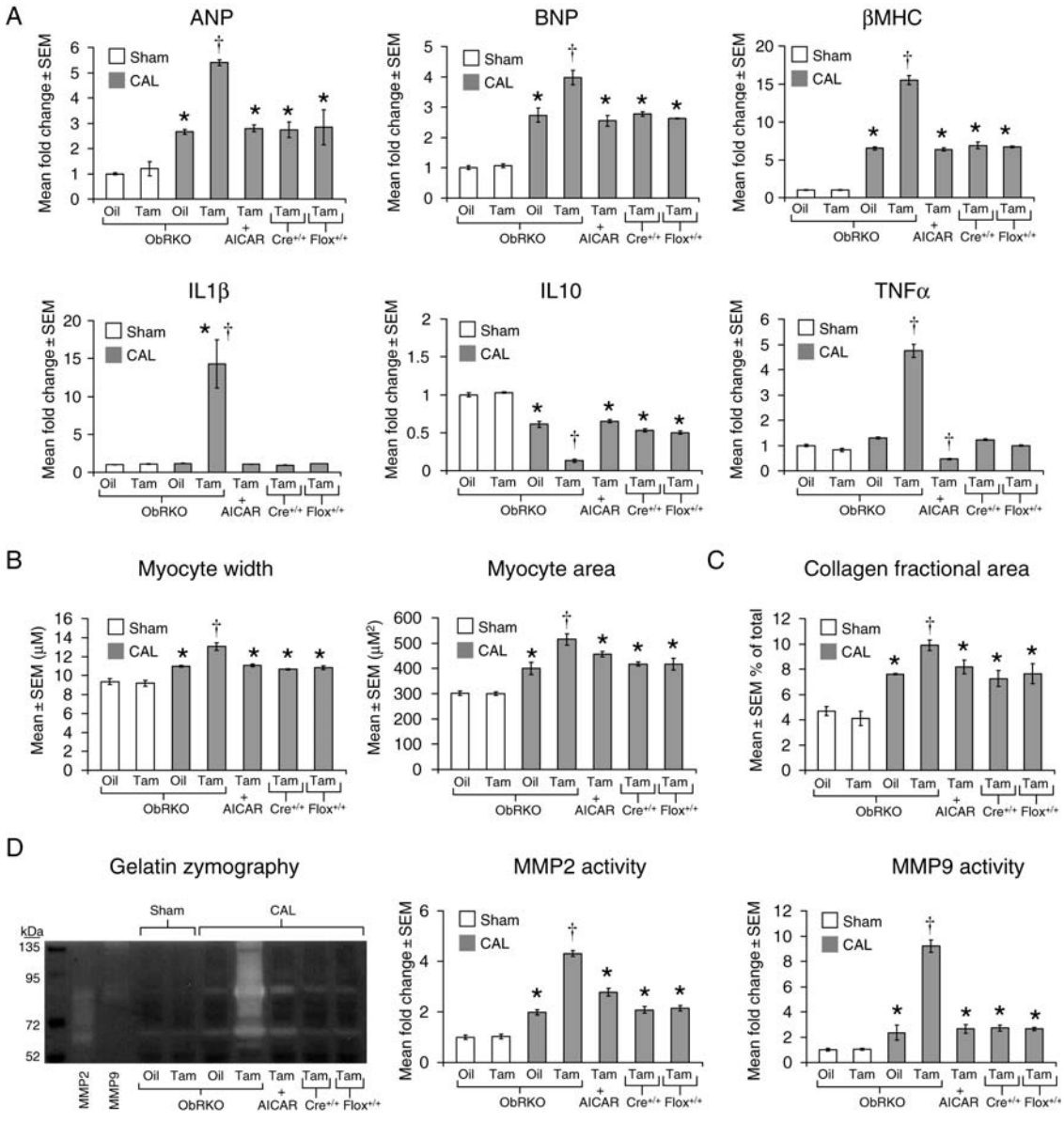

Figure 4 Tam-induced ObRKO mice demonstrate greater biochemical and histological measures of cardiac remodelling post-MI. $^{*}P < 0.05$ vs. shams and $^{\dagger}P < 0.05$ vs. all CAL groups. (*A*) Mean ± SEM fold change in cardiac ANP, BNP, βMHC, IL-1β, IL-10, and TNFα mRNAs in various groups of ObRKO and homozygous (+/+) parental MerCreMer ($Cre^{+/+}$) and floxed ($flox^{+/+}$) mice is shown. (*B*) Mean ± SEM myocyte width (left panel) and cross-sectional area (right panel) are shown. (*C*) Mean ± SEM per cent collagen area is shown. (*D*) Mean ± SEM fold change in cardiac MMP2 and 9 activities is shown (right), along with a representative zymogram (left).

0.05), and TUNEL/α-actinin positive (~0.29 vs. ~0.07%; $P < 0.05$) cells. Similarly, infarcted tissue from tam-treated ObRKO mice subjected to CAL demonstrated significantly greater levels of total TUNEL-positive (~3 vs. ~0.48%; $P < 0.05$), CD45-positive (~50 vs. ~32%; $P < 0.05$), and TUNEL/α-actinin-positive cells (~1.8 vs. ~0.22%; $P < 0.05$). Moreover, and consistent with histological data, a ~1.7-fold increase in caspase-3 activity was seen in oil-treated ObRKO mice subjected to CAL relative to shams ($P < 0.05$), with an additional increase to approximately three-fold in tam-treated ObRKO mice post-CAL ($P < 0.05$; *Figure 5G*; see Supplementary material online, *Figure S7*). In these *in vitro* experiments, caspase-3 activities in tam-treated homozygous (+/+) MerCreMer ($Cre^{+/+}$) and floxed ($flox^{+/+}$) parental mice subjected to CAL were not significantly different from vehicle-treated ObRKO mice (*Figure 5G*). With AICAR administration, significant reductions in total apoptosis, inflammation, TUNEL/α-actinin-positive cells, and caspase-3 activity were seen in tam-treated ObRKO mice at 1-month post-MI (*Figure 5A–G*).

3.6 Cardiac-specific reduction in ObR expression results in impaired glycolytic metabolism that is rescued with AMPK activation at 1-month post-MI

Post-MI, cardiac glycolysis was increased in oil-treated ObRKO mice and tam-treated homozygous (+/+) MerCreMer ($Cre^{+/+}$) and

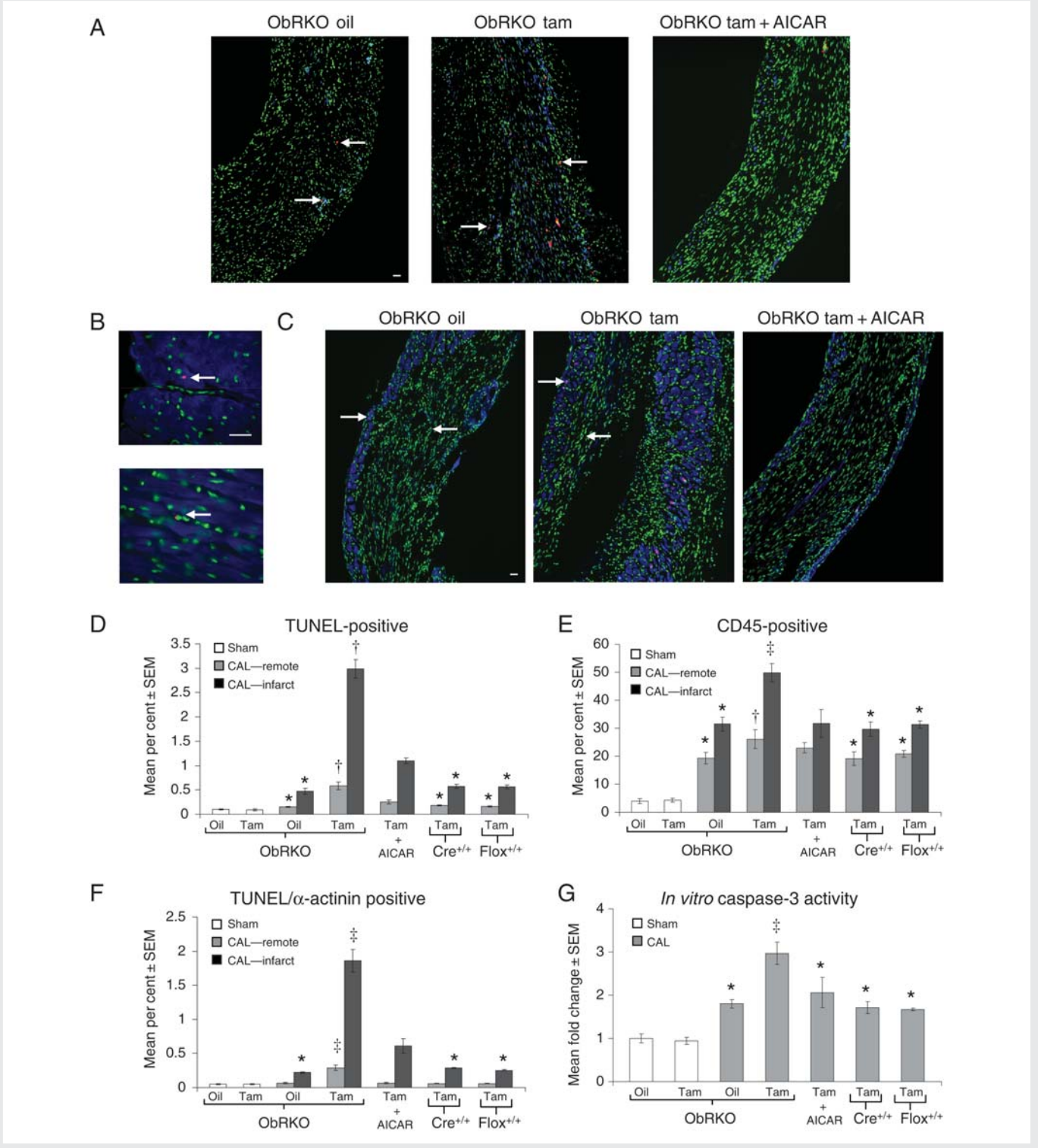

Figure 5 Tam-induced ObRKO mice demonstrate increased cardiac apoptosis, inflammation, and caspase-3 activity post-MI in both remote and infarcted myocardium. $^{*}P < 0.05$ vs. shams, $^{\dagger}P < 0.05$ vs. shams and all remote CAL groups, and $^{\ddagger}P < 0.05$ vs. all groups. (*A*) Representative ×20 power immunofluorescent TUNEL (in red, examples indicated by left facing arrows) and CD45 (in blue, examples indicated by right facing arrows) staining in infarcted tissue from ObRKO mice treated with oil, tam, and tam + AICAR. Nuclei (stained with DAPI) are shown in green, and accompanying scale bar (10 μM) is shown in white. (*B*) Representative ×60 power immunofluorescent TUNEL (in red, examples indicated by left facing arrows) and α-actinin (in blue) co-staining (top image), along with TUNEL positive/α-actinin negative staining (bottom image), in cardiac sections from ObRKO mice. Nuclei (stained with DAPI) are shown in green, and accompanying scale bar (10 μM) is shown in white. (*C*) As in (*A*), except that α-actinin-positive cells (rather than CD45-positive cells) were stained and are shown in blue. (*D*) Mean ± SEM apoptotic index in oil-treated and tam-induced sham and CAL ObRKO mice, and in tam-treated homozygous (+/+) parental MerCreMer ($Cre^{+/+}$) and floxed ($flox^{+/+}$) mice. (*E*) As in (*D*), except that mean ± SEM inflammatory index is shown. (*F*) As in (*D*), except that the mean ± SEM per cent TUNEL-positive/α-actinin-positive cells are shown. (*G*) As in (*D*), except that the mean ± SEM fold change in caspase-3 activity is shown.

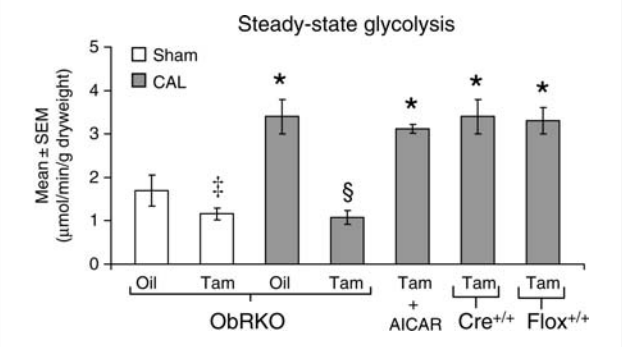

Figure 6 Tam-induced ObRKO mice demonstrate reduced steady-state rates of glycolysis that can be rescued with AICAR. Mean ± SEM steady-state rate of glycolysis (in μmol/min/g dry heart weight) in oil-treated and tam-induced sham and CAL ObRKO mice, in tam-treated homozygous (+/+) parental MerCre-Mer ($Cre^{+/+}$) and floxed ($flox^{+/+}$) mice, and in tam-induced CAL ObRKO mice administered AICAR. See Section 2 for *n* per group. $^{*}P < 0.05$ vs. shams, $^{‡}P < 0.05$ vs. oil-treated sham, and $^{§}P < 0.05$ vs. oil sham and all other CAL groups.

floxed ($flox^{+/+}$) parental mice, relative to shams (*Figure 6*). In tam-treated ObRKO mice, glycolytic rate was significantly impaired in both sham and infarcted hearts, and complete rescue was seen in CAL mice after AICAR administration (*Figure 6*).

4. Discussion

Here, we establish that leptin has a direct effect on the heart by demonstrating that cardiomyocyte-restricted loss of leptin signalling results in worse cardiac structure, function, and survival relative to wild-type mice after experimental MI, consistent with our previous observations in the whole-body leptin-deficient Ob/Ob mouse.[2,11] We go on to demonstrate that intact cardiac leptin signalling in ischaemic heart failure is important for the maintenance of glycolytic metabolism, involves the activation of STAT3 and AMPK, and is associated with attenuated indices of inflammation, apoptosis, and adverse cardiac remodelling post-MI. By demonstrating improvement in many exacerbated indices of cardiac structure and function that occur in the tam-treated ObRKO mouse post-MI with AICAR, we mechanistically link the cardioprotective benefit of leptin signalling to AMPK. Taken together, these results provide potential mechanisms by which intact leptin signalling improves outcomes in ischaemic heart failure.

In the present study, experiments using the ObRKO mouse demonstrate the relative importance of cardiac vs. non-cardiac leptin signalling in the ischaemic failing heart and suggest a compensatory role for the increased ObR expression that occurs in wild-type mice post-MI[2,20] and in humans with heart failure.[3] Specifically, in ObRKO mice with reduced cardiac ObR expression, a corresponding loss of STAT3 and AMPK activation is seen in the failing heart. The importance of this finding is that STAT3 and AMPK activation mitigates cardiac ischaemic injury. For example, in mice with a loss of STAT3 activation, greater adverse left ventricular remodelling [21] and increased apoptosis[22] occur post-MI. Similarly, in mice expressing the kinase inactive form of AMPK, ischaemic glucose uptake and glycolysis are impaired, and post-ischaemic cardiac function and apoptosis are exacerbated.[23] Our results using the ObRKO mouse are consistent with these[21–23] published reports and demonstrate that a loss of cardiac STAT3 and AMPK activation in the ischaemic failing heart is linked to increased levels of adverse structural, functional, biochemical, and metabolic remodelling.

Our data demonstrate that excision of the ObR gene has no effect on the basal activation state of STAT3 or AMPK, or on myocardial structure or contractile performance during a short (4 week) period of observation. Indeed, data from Ob/Ob and Db/Db mice suggest that longer perturbation of ObR signalling is required to see changes in cardiac structure and function under basal conditions[5] and that ischaemic injury[2,24] accelerates this process. Combined, these *in vivo* data[2,5,24] are in contrast to several,[25–27] but not all,[28] *in vitro* studies reporting that leptin can induce hypertrophy in cultured rat neonatal or human paediatric cardiomyocytes. Reasons for these varied *in vivo* vs. *in vitro* responses may be due to a number of factors, including the reported lack of long-form ObR expression in rat neonatal cardiomyocytes,[26] the lack of non-cardiomyocyte cells in culture preparations that secrete factors such as angiotensin-(1–7)[29] and interferon-γ[30] that mediate anti-hypertrophic effects, the loss of extracellular matrix (ECM) that provides and/or alleviates varied degrees of wall stress *in vivo*,[31] and the different culture conditions under which experiments were performed. The acute effect of leptin administration may also be different than the chronic effect of deficiency. In particular, it has been proposed that the age-related hypertrophy observed in Ob/Ob and Db/Db mice is a consequence of many deranged physiological parameters that occur in these mice over time and is not a direct consequence of leptin deficiency *per se*.[25] Although our data do not directly address the issue of age-related hypertrophy in states of leptin deficiency, we do demonstrate using our cardiac-specific ObR knockout mouse that the mitigating effects of leptin on post-MI hypertrophy are specific to cardiac tissue and not dependent on any systemic actions of leptin. Thus, although final conclusions regarding leptin-mediated cardiomyocyte hypertrophy based on *in vitro* data remain to be clarified, our data suggest that impaired cardiac leptin signalling post-MI results in a decrease in AMPK activity and an increase in cardiomyocyte hypertrophy.

Cardiomyocyte hypertrophy can develop as a compensatory response to increases in cardiac pressure and/or volume. However, with time, hypertrophy leads to cardiac failure, characterized by maladaptive remodelling of the ECM, reduced contractile performance, and ventricular dilation. Inflammation plays a role in regulating ECM remodelling by contributing to alterations in cardiac MMP activity and collagen deposition.[31] Specifically, mast cells within the myocardium release a variety of factors, including TNFα, that increase MMP expression and activation,[32] and evidence suggests that both neutrophils and macrophages secrete and activate MMPs in the post-MI heart.[33] Consistent with these observations, we show increased cardiac MMP activity, collagen deposition, inflammatory cytokine expression (including TNFa), and increased inflammatory cell infiltrates in tam-treated ObRKO mice post-MI. Further, we demonstrate a reduction in these measures with AICAR administration, suggesting the involvement of AMPK. This is consistent with other reports[34,35] demonstrating that AMPK modulates inflammatory responses. In particular, AMPK not only suppresses pro-inflammatory responses in macrophages,[34] but it also inhibits the production and activity of pro-inflammatory cytokines such as TNFa.[35] Thus, impaired cardiac leptin signalling post-MI is linked to decreased AMPK

activation and increased maladaptive cardiac remodelling characterized by exacerbated inflammation, collagen deposition, and MMP activity.

In addition to increased inflammation, we also show increased cardiomyocyte apoptosis post-MI in tam-treated ObRKO mice that is rescued with AICAR. Our findings complement reported rates of cardiac apoptosis seen in Ob/Ob and Db/Db mice with ageing[6] and extend the results of our previous study which demonstrated increased cardiac apoptosis post-MI in both lean and obese Ob/Ob mice.[11] Specifically, we now not only show the increased apoptotic cell number in mice with impaired cardiac leptin signalling post-MI, but also demonstrate that the majority of cells undergoing apoptosis in both remote and infarcted regions stain with the cardiomyocyte-specific marker α-actinin. Mechanistically, our experiments with AICAR demonstrate the involvement of AMPK and are consistent with studies showing AMPK-mediated protection from hypoxia/reoxygenation-,[36] TNFα-,[37] and ischaemia/reperfusion[23]-induced cardiac apoptosis. We speculate that complete normalization of apoptotic rates was not achieved in our study, however, due to either the relatively short duration of AICAR administration, and/or the involvement of additional leptin-dependent, but AMPK-independent, anti-apoptotic factors and pathways. For example, in addition to AMPK,[36] evidence suggests that leptin attenuates apoptosis in cardiac cells through the activation of p38 mitogen-activated kinase,[36] phosphoinositide 3-kinase,[38] and STAT3.[11] Nevertheless, our experiments using AICAR confirm a mechanistic link and demonstrate a unique AMPK-dependent anti-apoptotic role for leptin in the ischaemic failing heart.

Our data demonstrate that leptin impacts hypertrophy, collagen deposition, MMP activity, inflammation, and apoptosis in the ischaemic failing heart and thereby plays an important role in mitigating adverse structural remodelling post-MI. Another major finding in this study is that leptin also mediates metabolic remodelling in ischaemic heart failure. Specifically, we demonstrate increased glycolysis post-MI only in hearts with intact leptin signalling and reduced glycolytic rates in mice with impaired leptin signalling that can be rescued with AICAR. These results are in agreement with findings in Ob/Ob and Db/Db mice that show a reduction in cardiac glucose utilization and contractile function that precede the development of obesity and hyperglycaemia.[7,39] Given these observations, it is likely that the reduction in anaerobic metabolism we see in hearts with impaired leptin signalling is a major contributing factor to the accentuated impairments we see in LV systolic function, cardiac output, stroke work, and contractility (dP/dt_{max}) in the tam-treated ObRKO mouse post-MI. Indeed, independent of leptin, studies consistently demonstrate a significant reduction in cardiac mechanical efficiency when free fatty acids are used preferentially over glucose for energy production in the failing heart.[40] Our data demonstrating restoration of glycolysis and significant improvements in cardiac function with AICAR treatment suggest a direct link between leptin-mediated glycolytic metabolism and cardiac function post-MI, and highlight the dependence on AMPK in the process.

In conclusion, our data show that leptin mitigates heart failure post-MI by acting directly on the cardiomyocyte to increase ObR signalling and decrease cardiac hypertrophy, apoptosis, and inflammation. Further, our results demonstrate that intact cardiac leptin signalling is an important mediator of anaerobic metabolism which occurs in the ischaemic failing heart and is associated with less severe decrements in cardiac function and apoptosis post-MI. Together, these observations complement studies reporting increased circulating leptin acutely after MI[9] and increased cardiac ObR expression[3] and circulating leptin[10] in human heart failure, by establishing a cardiomyocyte-specific role for leptin to improve outcomes in cardiac ischaemic injury.

Supplementary material

Supplementary material is available at *Cardiovascular Research* online.

Acknowledgements

We acknowledge the assistance of the CBI at the University of Pittsburgh in providing access to microscopy equipment.

Conflict of interest: none declared.

Funding

This work was supported by the National Institutes of Health grants (HL-087009 to K.R.M., DK-072162 to R.M.O., and HL-077785 to C.P.O.), the Great Rivers Affiliate of the American Heart Association Beginning Grant-in-Aid (0865432D to K.R.M.), and the Cardiovascular Institute at the University of Pittsburgh Medical Center.

References

1. Shuldiner AR, Yang R, Dong DW. Resistin, obesity, and insulin resistance: the emerging role of the adipoctye as an endocrine organ. *N Engl J Med* 2001;**345**:145–146.
2. McGaffin KR, Sun CK, Rager JJ, Romano LC, Zou B, Mathier MA *et al*. Leptin signalling reduces the severity of cardiac dysfunction and remodelling after chronic ischaemic injury. *Cardiovasc Res* 2008;**77**:54–63.
3. McGaffin KR, Moravec CS, McTiernan CF. Leptin signaling in the failing and mechanically unloaded human heart. *Circ Heart Fail* 2009;**2**:676–683.
4. Minhas K, Khan SA, Raju SV, Phan AC, Gonzalez DR, Skaf MW *et al*. Leptin repletion restores depressed {beta}-adrenergic contractility in ob/ob mice independently of cardiac hypertrophy. *J Physiol* 2005;**565**:462–474.
5. Barouch LA, Berkowitz DE, Harrison RW, O'Donnell CP, Hare JM. Disruption of leptin signaling contributes to cardiac hypertrophy independently of body weight in mice. *Circulation* 2003;**108**:754–759.
6. Barouch LA, Gao D, Lei C, Miller KL, Xu W, Phan AC *et al*. Cardiac myocyte apoptosis is associated with increased DNA damage and decreased survival in murine models of obesity. *Circ Res* 2006;**98**:119–124.
7. Mazumder PK, O'Neill BT, Roberts MW, Buchanan J, Yun UJ, Cooksey RC *et al*. Impaired cardiac efficiency and increased fatty acid oxidation in insulin-resistant ob/ob mouse hearts. *Diabetes* 2004;**53**:2366–2374.
8. Panagia M, Schneider JE, Brown B, Cole MA, Clarke K. Abnormal function and glucose metabolism in the type-2 diabetic db/db mouse heart. *Can J Physiol Pharmacol* 2007;**85**:289–294.
9. Meisel SR, Ellis M, Pariente C, Pauzner H, Liebowitz M, David D *et al*. Serum leptin levels increase following acute myocardial infarction. *Cardiology* 2001;**95**:206–211.
10. Schulze PC, Kratzsch J, Linke A, Schoene N, Adams V, Gielen S *et al*. Elevated serum levels of leptin and soluble receptor in patients with advanced chronic heart failure. *Eur J Heart Fail* 2003;**5**:33–40.
11. McGaffin KR, Zou B, McTiernan CF, O'Donnell CP. Leptin attenuates cardiac apoptosis after chronic ischaemic injury. *Cardiovasc Res* 2009;**83**:313–324.
12. Dolinsky V, Dyck JR. Role of AMP-activated protein kinase in healthy and diseased hearts. *Am J Physiol Heart Circ Physiol* 1006;**291**:H2557–H2569.
13. Cohen P, Zhao C, Cai X, Montez JM, Rohani SC, Feinstein P *et al*. Selective deletion of leptin receptor in neurons leads to obesity. *J Clin Invest* 2001;**108**:1113–1121.
14. Naghshin J, McGaffin KR, Witham WG, Mathier MA, Romano LC, Smith SH *et al*. Chronic intermittent hypoxia increases left ventricular contractility in C57BL/6J mice. *J Appl Physiol* 2009;**107**:787–793.
15. Lopaschuk GD, Barr RL. Measurements of fatty acid and carbohydrate metabolism in the isolated rat heart. *Mol Cell Biochem* 1997;**172**:137–147.
16. Koitabashi N, Bedja D, Zaiman AL, Pinto YM, Zhang M, Gabrielson KL *et al*. Avoidance of transient cardiomyopathy in cardiomyocyte-targeted tamoxifen-induced MerCreMer gene deletion models. *Circ Res* 2009;**105**:12–15.
17. Fruhbeck G. Intracellular signaling pathways activated by leptin. *Biochem J* 2006;**393**:7–20.
18. Li H-L, Yin R, Chen D, Liu D, Wang D, Yang Q *et al*. Long-term activation of adenosine monophosphate-activated protein kinase attenuates pressure-overload-induced cardiac hypertrophy. *J Cell Biochem* 2007;**100**:1086–1099.

19. Russell RR, Bergerson R, Shulman GI, Young L. Translocation of myocardial glut-4 and increased glucose uptake through activation of AMPK by AICAR. *Am J Heart Circ Physiol* 1999;**277**:643–649.
20. Matsui H, Motooka M, Koike H, Inoue M, Iwasaki T, Suzuki T *et al*. Ischemia/reperfusion in rat heart induces leptin and leptin receptor gene expression. *Life Sci* 2007;**80**: 672–680.
21. Krishnamurthy P, Rajasingh J, Lambers E, Qin G, Losordo DW, Kishore R. IL-10 inhibits inflammation and attenuates left ventricular remodeling after myocardial infarction via activation of STAT3 and suppression of HuR. *Circ Res* 2009;**104**:e9–e18.
22. Hilfiker-Kleiner D, Hilfiker A, Drexler H. Many good reasons to have STAT3 in the heart. *Pharmacol Ther* 2005;**107**:131–137.
23. Russell R, Li J, Coven DL, Pypaert M, Zechner C, Palmeri M *et al*. AMP-activated protein kinase mediates ischemic glucose uptake and prevents postischemic cardiac dysfunction, apoptosis, and injury. *J Clin Invest* 2004;**114**:495–503.
24. Greer JJ, Ware DP, Lefer DJ. Myocardial infarction and heart failure in the db/db diabetic mouse. *Am J Physiol Heart Circ Physiol* 2006;**290**:H146–H153.
25. Madani S, De Girolamo S, Munoz DM, Li RK, Sweeney G. Direct effects of leptin on size and extracellular matrix components of human pediatric ventricular myocytes. *Cardiovasc Res* 2006;**69**:716–725.
26. Rajapurohitam V, Gan XT, Kirshenbaum LA, Karmazyn M. The obesity-associated peptide leptin induces hypertrophy in neonatal rat ventricular myocytes. *Circ Res* 2003;**93**:277–279.
27. Xu FP, Chen MS, Wang YZ, Yi Q, Lin SB, Chen AF *et al*. Leptin induces hypertrophy via endothelin-1-reactive oxygen species pathway in cultured neonatal rat cardiomyocytes. *Circulation* 2004;**110**:1269–1275.
28. Pinieiro R, Iglesias M, Eiras S, Vinuela J, Lago F, Gonzales-Juanatey JR. Leptin does not induce hypertrophy, cell cycle alterations, or production of MCP-1 in cultured rat and mouse cardiomyocytes. *Endocr Res* 2005;**31**:375–386.
29. Iwata M, Cowling RT, Gurantz D, Moore C, Zhang S, Yuan JX *et al*. Angiotensin-(1-7) binds to specific receptors on cardiac fibroblasts to initiate antifibrotic and antihypertrophic effects. *Am J Physiol Heart Circ Physiol* 2005;**289**:H2356–H2363.
30. Jin H, Li W, Yang R, Ogasawara A, Lu H, Paoni NF. Inhibitory effects of interferon-gamma on myocardial hypertrophy. *Cytokine* 2005;**31**:405–414.
31. Hutchinson KR, Stewart JA, Lucchesi PA. Extracellular matrix remodeling during the progression of volume overload-induced heart failure. *J Mol Cell Card* 2010;**48**: 564–569.
32. Janicki JS, Brower GL, Gardner JD, Chancey AL, Stewart JA. The dynamic interaction between matrix metalloproteinase activity and adverse myocardial remodeling. *Heart Failure Reviews* 2004;**9**:33–42.
33. Tao ZY, Cavasin MA, Yang F, Liu YH, Yang XP. Temporal changes in matrix metalloproteinase expression and inflammatory response associated with cardiac rupture after myocardial infarction in mice. *Life Sci* 2004;**74**:1561–1572.
34. Sag D, Cardling D, Stout RD, Suttles J. Adenosine 5′-monophosphate-activated protein kinase promotes macrophage polarization to an anti-inflammatory phenotype. *J Immunol* 2008;**181**:8633–8641.
35. Nath N, Giri S, Prasad R, Salem ML, Singh AK, Singh I. 5-Aminoimidazole-4-carboxamide ribonucleoside: a novel immunomodulator with therapeutic efficacy in experimental autoimmune encephalomyelitis. *J Immunol* 2005;**175**:566–574.
36. Shin EJ, Schram K, Zheng XL, Sweeny G. Leptin attenuates hypoxia/oxygen-induced activation of the intrinsic pathway of apoptosis in rat H9c2 cells. *J Cell Physiol* 2009; **221**:490–497.
37. Kewalramani G, Puthanveetil P, Wang F, Kim MS, Deppe S, Abrahani A *et al*. AMP-activated protein kinase confers protection against TNF-alpha-induced cardiac cell death. *Cardiovasc Res* 2009;**84**:42–53.
38. Trivedi P, Yang R, Barouch LA. Decreased p110a catalytic activity accompanies increased myocyte apoptosis and cardiac hypertrophy in leptin deficient ob/ob mice. *Cell Cycle* 2008;**7**:560–565.
39. Buchanan J, Mazumder PK, Ping H, Chakrabarti G, Roberts MW, Yun UJ *et al*. Reduced cardiac efficiency and altered substrate metabolism preceded the onset of hyperglycemia and contractile dysfunction in two mouse models of insulin resistance and obesity. *Endocrinology* 2005;**146**:5341–5349.
40. Lopaschuk GD, Ussher J, Folmes CD, Jaswal JS, Stanley WC. Myocardial fatty acid metabolism in health and disease. *Physiol Rev* 2010;**90**:207–258.